Application of Homogeneous Potentials for the Modeling of the Bauschinger Effects in Ultra Low Carbon Steel

Jin-Jin Ha, Jin-Woo Lee, Toshihiko Kuwabara, Myoung-Gyu Lee, and Frédéric Barlat

Citation: AIP Conference Proceedings **1353**, 1453 (2011); doi: 10.1063/1.3589721
View online: http://dx.doi.org/10.1063/1.3589721
View Table of Contents: http://scitation.aip.org/content/aip/proceeding/aipcp/1353?ver=pdfcov
Published by the AIP Publishing

Application of Homogeneous Potentials for the Modeling of the Bauschinger Effects in Ultra Low Carbon Steel

Jin-Jin Ha[a], Jin-Woo Lee[a], Toshihiko Kuwabara[b],
Myoung-Gyu Lee[a], Frédéric Barlat[a]

[a]*Graduate Institute of Ferrous Technology (GIFT), Pohang University of Science and Technology (POSTECH), San 31 Hyoja-dong, Nam-gu, Pohang, Gyeongbuk 790-784, Republic of Korea*
[b]*Division of Advanced Mechanical Systems Engineering, Graduate School of Tokyo University of Agriculture and Technology, 2-24-16, Naka-cho, Koganei-shi, Tokyo 184-8588, Japan*

Abstract. In this work, an approach is proposed for the description of the plastic behavior of materials subjected to multiple or continuous strain path changes. In particular, although it is not formulated with a kinematic hardening rule, it provides a reasonable description of the Bauschinger effect when loading is reversed. This description of anisotropic hardening is based on homogeneous yield functions/plastic potentials combining a stable, isotropic hardening-type, component and a fluctuating component. The capability of this constitutive description is illustrated with applications on an ultra low carbon steel sheet sample deformed in three-stage uniaxial loading with two load reversals [1].

Keywords: Bauschinger effect, Constitutive model, Reverse loading, Strain hardening, Yield function
PACS: 62.20.F

INTRODUCTION

In forming analyses, the description of the plastic behavior of a material is an important aspect to consider. For uniaxial deformation, the monotonic stress-strain curve is not always suitable when a material experiences non linear strain paths under specific process conditions. In particular, the Bauschinger effect is of interest when a load reversal occurs. This effect is characterized by a lower flow stress and a different hardening rate compared to the monotonic curve at the same accumulated plastic strain. Sheet metal forming simulations have shown that it plays an important role in the prediction of springback. Therefore, suitable descriptions of the uniaxial Bauschinger effect and their integrations into multiaxial constitutive models were proposed during the last decades [2, 3, 4]. In all these models, the Bauschinger effect is captured using a kinematic hardening rule in which the yield surface translates in stress space. The purpose of the present work is to propose an alternate formulation, which is based on homogeneous yield functions and does not involve kinematic hardening.

HAH MODEL

The Homogeneous yield function-based Anisotropic Hardening (HAH) model was formulated using the so-called microstructure deviator, $\hat{\mathbf{h}}^{\mathbf{s}}$, a state variable keeping track of the prior material deformation history [5]. Roughly, this tensor can be viewed as the continuum representation of a given set of active slip systems, irrespective of the slip direction, for a representative volume element of a polycrystal. For an undeformed material, this tensor is set equal to the stress deviator $\hat{\mathbf{s}}$ initiating plastic deformation. Then, $\hat{\mathbf{h}}^{\mathbf{s}}$ is governed by its own evolution equations described below, but this deviator is always normalized, i.e., $\hat{\mathbf{h}}^{\mathbf{s}} : \hat{\mathbf{h}}^{\mathbf{s}} = 3/8$, as indicated by the symbol "$\hat{\ }$". A yield function Φ is homogenous of degree a if, for any real λ, $\Phi(\lambda\mathbf{s}) = \lambda^a \Phi(\mathbf{s})$. In this work, a homogeneous function of degree 1, defined as a combination of a stable component ϕ and a fluctuating component ϕ_h, is proposed

The 14th International ESAFORM Conference on Material Forming
AIP Conf. Proc. 1353, 1453-1457 (2011); doi: 10.1063/1.3589721

$$\Phi(\mathbf{s}) = \left[\phi^q + \phi_h^q\right] = \left[\phi^q + f_1^q \left|\hat{\mathbf{h}}^s : \mathbf{s} - \left|\hat{\mathbf{h}}^s : \mathbf{s}\right|\right|^q + f_2^q \left|\hat{\mathbf{h}}^s : \mathbf{s} + \left|\hat{\mathbf{h}}^s : \mathbf{s}\right|\right|^q\right]^{\frac{1}{q}} = \bar{\sigma} \tag{1}$$

Any isotropic or anisotropic yield function ϕ, homogenous of an arbitrary degree, may be used as the stable component in this theory. However, it is first reduced to a yield function of degree one and written in the form of effective stress $\phi(\mathbf{s}) = \bar{\sigma}$. In the above equation, q is a constant exponent, while f_1 and f_2 are defined using two state variables g_1 and g_2

$$f_1 = \left[\frac{1}{g_1^q} - 1\right]^{\frac{1}{q}} \quad \text{and} \quad f_2 = \left[\frac{1}{g_2^q} - 1\right]^{\frac{1}{q}} \tag{2}$$

g_1 and g_2 correspond to the relative intensity of the stress compared to isotropic hardening, e.g., $\mathbf{s} = g_k \mathbf{s}_{\mathbf{iso}}$ (see Fig. 1), where $k = 1$ or 2 depending on the sign of $\mathbf{s} : \hat{\mathbf{h}}^s$ and $\mathbf{s}_{\mathbf{iso}}$ would be the active stress state if strain hardening was isotropic. One of the simplest evolution laws for these state variables are given by the following relationships

- If $\mathbf{s} : \hat{\mathbf{h}}^s \geq 0$
  - $\dfrac{dg_1}{d\bar{\varepsilon}} = k_2\left(k_3 \dfrac{\bar{\sigma}_0}{\bar{\sigma}} - g_1\right)$
  - $\dfrac{dg_2}{d\bar{\varepsilon}} = k_1 \dfrac{1 - g_2}{g_2}$ (3)
  - $\dfrac{d\hat{\mathbf{h}}^s}{d\bar{\varepsilon}} = k\left[\hat{\mathbf{s}} - \dfrac{8}{3}\hat{\mathbf{h}}^s\left(\hat{\mathbf{s}} : \hat{\mathbf{h}}^s\right)\right]$
- If $\mathbf{s} : \hat{\mathbf{h}}^s < 0$
  - $\dfrac{dg_1}{d\bar{\varepsilon}} = k_1 \dfrac{1 - g_1}{g_1}$
  - $\dfrac{dg_2}{d\bar{\varepsilon}} = k_2\left(k_3 \dfrac{\bar{\sigma}_0}{\bar{\sigma}} - g_2\right)$ (4)
  - $\dfrac{d\hat{\mathbf{h}}^s}{d\bar{\varepsilon}} = k\left[-\hat{\mathbf{s}} + \dfrac{8}{3}\hat{\mathbf{h}}^s\left(\hat{\mathbf{s}} : \hat{\mathbf{h}}^s\right)\right]$

where the coefficients k_1, k_2 and k_3 control the evolution of $g_1(\bar{\varepsilon})$ and $g_2(\bar{\varepsilon})$ in the effective strain $\bar{\varepsilon}$, i.e., the new flow stress and hardening rate after unloading and reloading, and k is associated to the rotation rate of the microstructure deviator.

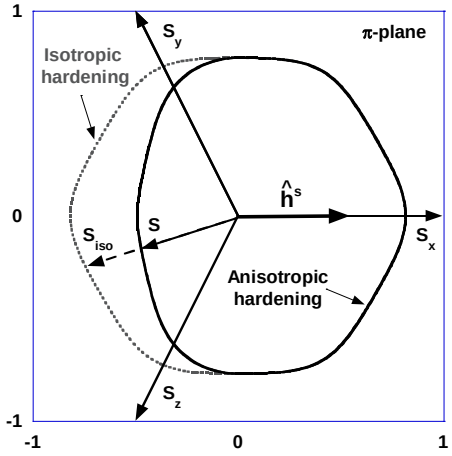

FIGURE 1. Normalized yield surfaces in the π-plane after isotropic and anisotropic hardening.

APPLICATION TO ULTRA LOW CARBON STEEL SHEET

In this application, the HAH approach was applied with the von Mises yield function and state variable evolutions based on a dislocation density model [6] giving a flow curve of the form

$$\bar{\sigma}(\bar{\varepsilon}) = M\left[\tau_0 + \alpha\mu b\sqrt{\rho(\bar{\varepsilon})}\right] \tag{5}$$

In the above relationship, $\rho(\bar{\varepsilon})$ is the dislocation density as a function of the accumulated plastic strain, which is defined using the plastic work equivalence principle, M is the Taylor factor, τ_0 the friction stress, α a constant, μ the shear modulus and b the Burgers vector. Additional variables were also introduced in order to capture a permanent softening effect [5]. All the state variable evolution equations for the HAH model with the corresponding coefficients are listed in the Appendix and in Tables 1 and 2. Monotonic tests as well as sequences tension-compression-tension (TCT) and compression-tension-compression (CTC) were conducted by Verma et al. [1] on an ultra low carbon steel. Experimental details were described by the authors.

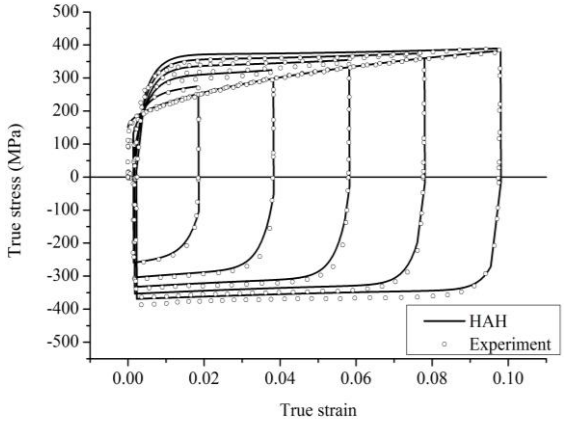

FIGURE 2. Experimental and simulated stress - strain curves in TCT for five different amounts of pre-strains.

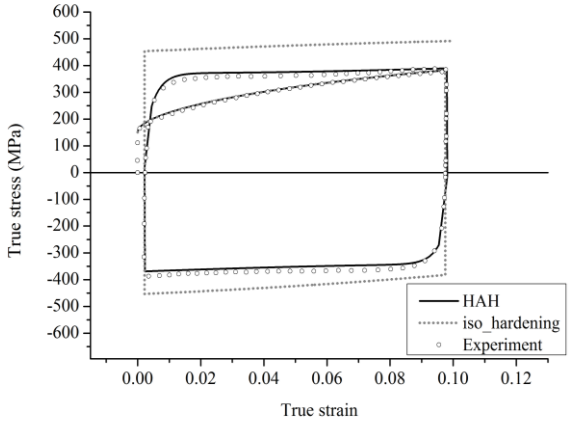

FIGURE 3. Comparison of stress – strain curves for the isotropic hardening and HAH models.

Figure 2 shows the calculated monotonic stress-strain curve, which was calibrated on the experimental data (coefficients in Table 1). The coefficients characterizing anisotropic strain hardening, which were calibrated using a tension-compression response with a strain reversal of 0.1, are listed in Table 2. This figure represents also the curves calculated for all the TCT sequences with reversal at strains of 0.02, 0.04, 0.06, 0.08 and 0.10. They are in good agreement with the experiments. Figure 3 compares the calculated responses given by the HAH model and the isotropic hardening model, showing that isotropic hardening overestimates the flow stress significantly after load reversal. Figure 4 shows the stress-strain curves predicted with the HAH model for the CTC sequences, using the coefficients determined with the TCT curve with reversal at a strain of 0.1. Again, a good agreement with experimental data was obtained.

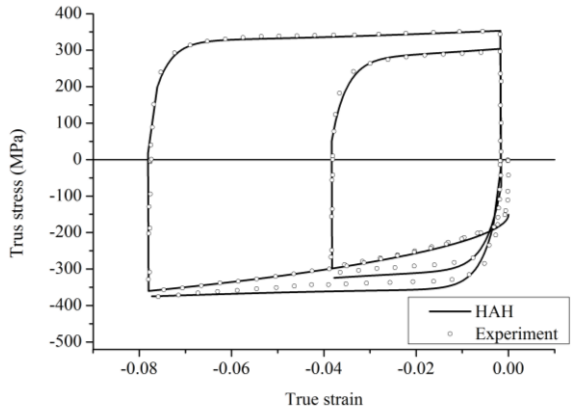

FIGURE 4. Experimental and simulated stress - strain curves of CTC for two different amounts of pre-strains.

Figure 5 shows the calculated stress-strain behavior for different non-proportional loading sequences, namely, tension followed by compression, tension followed by orthogonal tension and tension followed by tension at 45^{o} from the first direction. The former corresponds to conditions close to reverse loading while the latter corresponds to conditions close to cross-loading, i.e., for which the two stress deviators $\mathbf{s}_1$ and $\mathbf{s}_2$ are such that $\mathbf{s}_1 : \mathbf{s}_2 = 0$. In this figure, no experimental data are available. Figure 5 indicates that the reloading flow stress after reversal is lower than that after orthogonal tension. Moreover, the flow stress after reloading at 45^{o} is the same as that just before unloading. These predicted results agree generally well with experimental trends reported in the literature, as for instance, in reference [7].

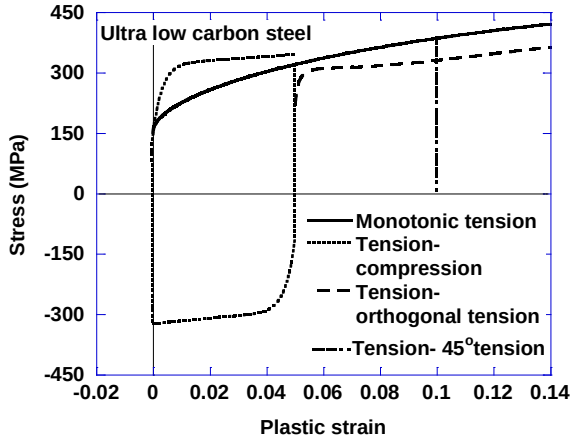

FIGURE 5. HAH calculated stress-strain curves for different strain paths.

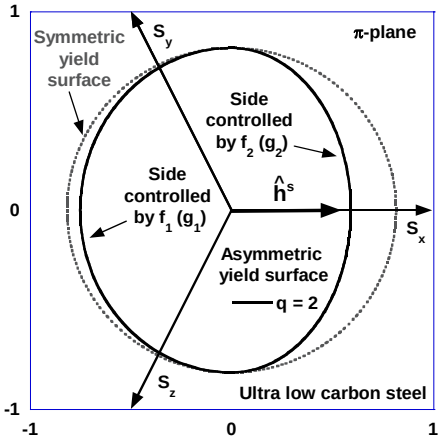

FIGURE 6. Isotropic and asymmetric yield loci after stress reversal

Finally, Figure 6 is a snapshot of the yield surface in the π-plane after tension up to a strain of 0.05, load reversal and compression up to a strain of 0.01. Compared to the yield surface obeying the isotropic hardening rule, denoted "symmetric yield surface" in this figure, the HAH yield surface is distorted (or asymmetric). This reflects the influence of the two loading stages, tension and compression, that were applied in direction $\mathbf{e}_x$.

CONCLUSIONS

Although the HAH model presented in this work is based on homogeneous yield functions, it can capture the main trends observed during strain path changes. The Bauschinger effect and the strain hardening behavior observed during tension-compression-tension (TCT) and compression-tension-compression (CTC) tests performed on low carbon steel were satisfactorily reproduced by a dislocation-density based state variable evolution. Although the examples shown in this article were based on von Mises plasticity, this approach can be used with any isotropic or anisotropic yield function. Further investigations are needed in the future in order to refine the theory, provide additional capabilities, further validate its predictive potential with other critical experiments, and implement the model in numerical forming simulation codes.

ACKNOWLEDGMENTS

This research was supported by POSCO and by the World Class University (WCU) program through the National Research Foundation of the Korean Ministry of Education, Science and Technology (Grant #R32-10147).

REFERENCES

1. R. K. Verma, T. Kuwabara, K. Chung, A. Haldar, *Int. J. Plasticity*, 27 (1), 82-101 (2011)
2. F. Yoshida, T. Uemori, K. Fujiwara, *Int. J. Plasticity*, 18, 633-659 (2002)

3. C. Teodosiu, Z. Hu, "Microstructure in the continuum modeling of plastic anisotropy", in *Proc. Risø International Symposium on Material Science: Modelling of Structure and Mechanics of Materials from Microscale to products*, edited by J.V. Cartensen, T. Leffers, T. Lorentzen, O.B. Pedersen, B.F. Sørensen, G. Winther, Risø National Laboratory, Roskilde, Denmark, 1998, pp. 149-168.
4. J. L. Chaboche, *Int. J. Plasticity*, 2(2), 149-188 (1986)
5. F. Barlat, J. J. Gracio, M. G. Lee, E. F. Rauch, G. Vincze, submitted to *Int. J. Plasticity* (2011)
6. E. F. Rauch, J. J. Gracio, F. Barlat, *Acta Materialia*, 55, 2939-2948 (2007)
7. D. J. Lloyd, H. Sang, *Metallurgical Transactions*, 10A, 1767-1772 (1979)

APPENDIX

The state variable evolution equations for the dislocation based model are given below. The simpler case, irrespective of permanent softening, described by (3) and (4) is recovered when $k_4 = 1$ or $k_5 = 0$ and $g_3 = g_4 = 1$:

- Case $\mathbf{s} : \hat{\mathbf{h}}^s \geq 0$
  - $\frac{dg_1}{d\bar{\varepsilon}} = k_2\left(k_3\frac{\bar{\sigma}_0}{\bar{\sigma}} - g_1\right)$
  - $\frac{dg_2}{d\bar{\varepsilon}} = k_1\frac{g_3 - g_2}{g_2}$
  - $\frac{dg_4}{d\bar{\varepsilon}} = k_5\left(k_4 - g_4\right)$
  - $\frac{d\hat{\mathbf{h}}^s}{d\bar{\varepsilon}} = k\left[\hat{\mathbf{s}} - \frac{8}{3}\hat{\mathbf{h}}^s\left(\hat{\mathbf{s}} : \hat{\mathbf{h}}^s\right)\right]$
  - $\frac{d\rho_{f_1}}{d\bar{\varepsilon}} = \frac{\sqrt{\rho_{f_1}}}{bK} + \frac{1}{bD} - \kappa\rho_{f_1}$
  - $\frac{d\rho_{r_1}}{d\bar{\varepsilon}} = -\left(\frac{\sqrt{\rho_{f_1}}}{bK} + \frac{1}{bD}\right)\frac{\rho_{r_1}}{\rho_{f_{01}}}$
  - $\rho_{f_2} = (1-p)\rho_{f_1} + \rho_{r_1}$
  - $\rho_{r_2} = p\rho_{f_1}$
  - $\rho_{f_{02}} = \rho_{f_1}$
  - $\rho(\bar{\varepsilon}) = \rho_{f_1} + \rho_{r_1}$
- Case $\mathbf{s} : \hat{\mathbf{h}}^s < 0$
  - $\frac{dg_1}{d\bar{\varepsilon}} = k_1\frac{g_4 - g_1}{g_1}$
  - $\frac{dg_2}{d\bar{\varepsilon}} = k_2\left(k_3\frac{\bar{\sigma}_0}{\bar{\sigma}} - g_2\right)$
  - $\frac{dg_3}{d\bar{\varepsilon}} = k_5\left(k_4 - g_3\right)$
  - $\frac{d\hat{\mathbf{h}}^s}{d\bar{\varepsilon}} = k\left[-\hat{\mathbf{s}} + \frac{8}{3}\hat{\mathbf{h}}^s\left(\hat{\mathbf{s}} : \hat{\mathbf{h}}^s\right)\right]$
  - $\frac{d\rho_{f_2}}{d\bar{\varepsilon}} = \frac{\sqrt{\rho_{f_2}}}{bK} + \frac{1}{bD} - \kappa\rho_{f_2}$
  - $\frac{d\rho_{r_2}}{d\bar{\varepsilon}} = -\left(\frac{\sqrt{\rho_{f_2}}}{bK} + \frac{1}{bD}\right)\frac{\rho_{r_2}}{\rho_{f_{02}}}$
  - $\rho_{f_1} = (1-p)\rho_{f_2} + \rho_{r_2}$
  - $\rho_{r_1} = p\rho_{f_2}$
  - $\rho_{f_{01}} = \rho_{f_2}$
  - $\rho(\bar{\varepsilon}) = \rho_{f_2} + \rho_{r_2}$

The different coefficients of the HAH model for the ultra low carbon steel are listed below in Table 1 and 2.

TABLE 1. Isotropic hardening coefficients for ultra low carbon steel

α	$\mu(GPa)$	$b(nm)$	$\tau_0(MPa)$	M	K	$D(\mu m)$	F	p
0.5	85	0.246	53	2.85	180	22	2.8	0.8

TABLE 2. Yield function exponents and anisotropic hardening coefficients

a	q	k	k_1	k_2	k_3	k_4	k_5
2 (von Mises)	2	30	290	50	0.3	0.85	12